International Journal of Sciences: Basic and Applied Research (IJSBAR)

ISSN 2307-4531
(Print & Online)

http://gssrr.org/index.php?journal=JournalOfBasicAndApplied

Development of High Resolution Precipitation Extreme Dataset Using Spatial Interpolation Methods and Geostatistics in South Sulawesi, Indonesia

Amsari Mudzakir Setiawan[a], Yonny Koesmaryono[b], Akhmad Faqih[c*], Dodo Gunawan[d]

[a b,c]*Post Graduate School of Applied Climatology, Bogor Agricultural University (IPB), Campus of IPB Darmaga, Bogor, 16680, West Java, Indonesia*

[d]*Indonesia Agency for Meteorology Climatology and Geophysics (BMKG), Jl Angkasa I No. 2 Kemayoran Jakarta Pusat, 10720, Indonesia*

[a]*Email: amsari.setiawan@bmkg.go.id*

[b]*Email: yonny_ipb@yahoo.com*

[c]*Email: akhmadfa@apps.ipb.ac.id*

[d]*Email: dodo.gunawan@bmkg.go.id*

Abstract

Consecutive Dry Days (CDD) is one of several precipitation extreme parameter suggested by Expert Team on Climate Change Detection and Indices (ETCDDI) to give a brief overview about climatic condition, especially related to climate change and drought occurrences. Daily precipitation data from observed Indonesia Agency for Meteorology, Climatology and Geophysics (BMKG) station network and Climate Hazzard group Infra-Red Precipitation with Station (CHIRPS) during 35 years (1981 – 2015) in South Sulawesi was used for CDD calculation. Three approaches were used for developing high resolution gridded (0.05^o x 0.05^o) precipitation extreme index over ungauged area, i.e. i) CHIRPS standardization with observed CDD (Std_CHIRPS); ii) spatial interpolation using nearest neighbours (NN) and invers distance weighted (IDW); and iii) geostatistics method using ordinary kriging (OK) and regression kriging (RK).

---

* Corresponding author.

Spatial and temporal assessments for each interpolation performance were done by applying leave one out cross validation method with actual CDD from observed station data. This study found that spatial and temporal distribution of CDD over the region are described by almost all interpolation methods, except Std_CHIRPS. Interpolation performance was reduced during La Niña periods or after El Niño years. Highest correlation coefficient value with lowest RMSE obtained by OK and RK. Nevertheless, RK shows closest standard deviation value compared to observation data. Better interpolation performance achieved by RK compare to another method for CDD in South Sulawesi.

Keywords: Consecutive Dry Days; drought; geostatistics; spatial interpolation; precipitation extreme.

1. Introduction

Climatic information related to precipitation extreme and drought generally constructed based on precipitation data from meteorological rainfall observation network [1,3]. Consecutive Dry Days (CDD) is one of several precipitation extreme parameter suggested by Expert Team on Climate Change Detection and Indices (ETCDDI) to give a brief overview about climatic condition, especially related to climate change and drought occurrences [4]. South Sulawesi is located in the centre of Indonesian Maritime Continent which has various elevation, spatially high precipitation variability and greatly influenced by global climate anomaly occurrence [5,7]. Unfortunately, this region is not covered by high network density and dense distribution of meteorological stations. The problem arises when the community or policy-makers request climate related information over area which not covered by observation network. To overcome this limitation, spatial interpolation for estimating meteorological parameter over those area could be performed [8,10].

El Niño Southern Oscillation (ENSO) as one of the largest global climate phenomenon can lead to rainfall deficit and drought for several places in Indonesia [11], such as South Sulawesi [12], Pamengpeuk [13] and Cilacap [14]. Spatial heterogeneity of climate variability between one to another region lead to different impact associated with global climate anomaly [11,15]. For this reason, spatially high-resolution climatic information is essential for climate anomaly impact assessments.

Utilization and application of remote sensing data from weather satellite or radar become suitable option for providing climate related information [16,18]. The superiority of remote sensing data in providing an atmospheric dynamics condition is the strongest considerations for using this data as important climate information resource. Nevertheless, further correction should be done by dealing with bias between the results of remote sensing output and ground observations data [19,20]. Gridded reanalysis data from various global climate models output are another valuable alternative resource for providing precipitation extreme and drought information [21]. Unfortunately, spatial resolution of the model output still relatively low compare to remote sensing data and need to be downscaled to point station data [21,23]. Blending observation and remote sensing data are then performed to obtain higher spatial resolution [17,24].

Spatial interpolation methods are important tool in order to predict and estimate the values at unmeasured points from observed locations, such as precipitation data which is very important for meteorological drought

information [8]. Climate Hazards Group Infrared Precipitation with Station data (CHIRPS) is valuable of data assimilation product based on land-only climatic precipitation database and involve three diverse types of information such as global climatology data, satellite estimates and gauged observations. Furthermore, this database concatenates all information from monthly precipitation climatology CHPClim (Climate Hazards Group Precipitation Climatology), quasi-global geostationary thermal infrared satellite observations, Tropical Rainfall Measuring Mission's (TRMM) 3B42 product, atmospheric precipitation model from NOAA CFS (Climate Forecast System), and various precipitation observations sources, including national or regional Meteorological Services [25]. Nevertheless, higher spatial resolution (0.05^o x 0.05^o) is the main difference of this dataset compared to another majority of the available global precipitation data that have 0.5° x 0.5° or lower spatial resolution [26,27], such as APHRODITE [28,29], TRMM's 3B43 [30] and E-OBS [31] which have a 0.25° x 0.25° resolution.

Various spatial interpolation techniques have been applied to weather and climate parameter in tropical maritime countries such as nearest neighbours (NN), inverse distance weighted (IDW), ordinary kriging (OK), universal or regression kriging (RK), kriging with external drift and cokriging [32,33]. Although several spatial interpolation techniques can be readily used, it is complicated to determine which one is the best estimator for the actual observations. The characteristics of dataset determine the interpolation technique performance. An interpolation method is suitable for some variables but not work for another's [32]. Nevertheless, those interpolation methods and its performance assessment are not yet applied to generate high resolution CDD dataset.

The purpose of this research was to develop high resolution precipitation extreme dataset, especially for ungauged area in South Sulawesi Indonesia using simple statistics approach using CHIRPS standardization with observed CDD, spatial interpolation method and geostatistics technique. Furthermore, spatio-temporal validation and assessment for each interpolation performance was applied using leave one out cross validation method with actual CDD from observed station data. There are several limitations of this research, such as less observational data on mountainous area for validation, relatively sparse observed spatial distribution station on northern part of study area, limited observational network data quality and availability.

2. Material and Method

2.1. Dataset

Daily precipitation data at 293 active observation station in South Sulawesi from Indonesia Agency for Meteorology, Climatology and Geophysics (BMKG) observation network station spanning on 44 years period (1972 – 2015) are collected for this study. This observation network located on various altitude (2 – 1549 meter above sea level), consist of various source type (i.e. rain gauge (Obs Gauge); Agricultural Meteorological stations (AgriMet); BMKG weather stations) and evenly distributed over South Sulawesi (Figure 1) region. Data quality control have been performed to select stations which are comply the following criteria: the data are available for 25 or more years; missing data only 10 % or less per year; and passed standard normal homogeneity test [34] on annual precipitation to confirm homogeneity.

Finally, only 23 stations are selected which satisfied these criteria (Table 1) and only 35 years period (1981 - 2015) to meet up CHIRPS data temporal availability. This data was used to calculate maximum number of consecutive days with daily precipitation amount < 1 mm (CDD) [4].

CHIRPS dataset (available from 1981) also used to calculate CDD for each grid covered on the study area with 0.05^{o} x 0.05^{o} horizontal resolution.

This gridded dataset was obtained from Climate Hazards Group/ The Department of Geography, University of California Santa Barbara

(ftp://ftp.chg.ucsb.edu/pub/org/chg/products/CHIRPS-2.0/).

This dataset used to make comparison with observed data and used as independen variable to create trend model prediction during regression kriging analysis.

CDD are calculated from station and gridded data for each year over 35 years (1981 – 2015 period).

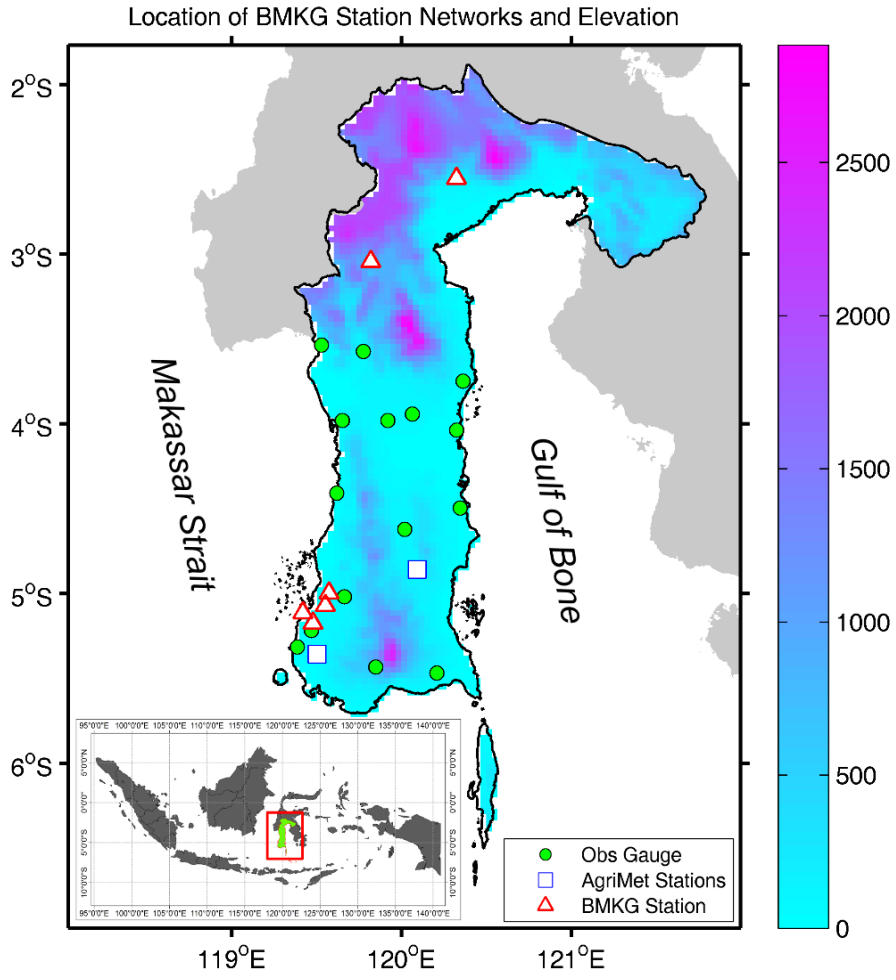

Figure 1: Spatial distribution of BMKG station networks with shaded elevation (in meter above sea level)

Table 1: List of BMKG observational network used for this study

Observed Station	Location	Altitude (m.a.s.l)	Type	Longitude	Latitude
ANABANUA	Wajo	15	Obs Gauge	120.06464	-3.94342
BATUBASSI	Maros	13	Obs Gauge	119.66269	-5.01972
BATUKAROPA	Bulukumba	81	AgriMet	120.20811	-5.46919
BIRINGROMANG	Makassar	8	BMKG	119.47931	-5.17575
BPPBENGO	Bone	77	Obs Gauge	120.02008	-4.62333
BPPDOPING	Wajo	4	Obs Gauge	120.32411	-4.03861
BPPKGALESONG	Takalar	15	Obs Gauge	119.38639	-5.31550
BPPMALAKAJI	Gowa	750	Obs Gauge	119.84842	-5.43408
BUKITHARAPAN	Pare-pare	80	Obs Gauge	119.65094	-3.98203
ENREKANG	Enrekang	65	Obs Gauge	119.77425	-3.57556
MACOPE	Bone	9	Obs Gauge	120.34703	-4.49661
MENGE	Wajo	38	Obs Gauge	119.91892	-3.98178
PGCAMMING	Bone	132	AgriMet	120.09275	-4.85911
PGTAKALAR	Takalar	15	AgriMet	119.50108	-5.35769
SIWA	Wajo	25	Obs Gauge	120.36394	-3.74975
STAKLIMMAROS	Maros	13	BMKG	119.57219	-4.99775
STAMARPAOTERE	Makassar	2	BMKG	119.41983	-5.11375
STAMETHASANUDDIN	Maros	14	BMKG	119.55214	-5.07100
STAMETMASAMBA	Luwu utara	50	BMKG	120.32417	-2.55444
STAMETPONGTIKU	Tana toraja	829	BMKG	119.81878	-3.04511
STASIUNGEOFISIKA	Gowa	28	Obs Gauge	119.46997	-5.21797
SUMPANGBINANGAE	Barru	7	Obs Gauge	119.61878	-4.40919
TODOKKONG	Pinrang	18	Obs Gauge	119.52875	-3.53786

2.2. Method

Simple statistics approach performed on CDD CHIRPS data by standardization with observed station data [35]. The standardization method applied for correcting climatological value and standard deviation by changing the origin and scaling the CDD data obtained from CHIRPS (Equation 1).

$$Std\_CHIRPS_i = (CDD_{CHIRPS,i} - m_{x,I}) * [(\delta_{y,i}/ \delta_{x,i}) + m_{y,i} \quad (1)$$

Here, Std_CHIRPS_i represent the corrected value and $CDD_{CHIRPS,i}$ for non-corrected value of the CHIRPS CDD of the i^{th} year. Where $m_{x,i}$ represent the spatial average of the CHIRPS with $\delta_{x,i}$ spatial standard deviation and $m_{y,i}$ is observed CDD with $\delta_{y,i}$ spatial standard deviation.

Almost all spatial interpolation methods estimations can be represented as weighted averages of sampled data

and used similar general estimation formula, as follows [36,37]:

$$\hat{z}(x_0) = \sum_{i=1}^{n} \lambda_i z(x_i) \quad (2)$$

Here, $\hat{z}$ is the estimated value of a parameter at the unmeasured location x_0, z is observed value at the sampled point x_i, λ_i is the weight assigned to the sampled point, and n represents the number of sampled points used for the estimation. The nearest neighbours (NN) is one of the earliest and simplest method. This method estimates the parameter value at an unmeasured point based on the value of the nearest sample by drawing perpendicular bisectors between sampled points (n), forming such as Thiessen (or Dirichlet/Voronoi) polygons (V_i, i=1, 2, 3, …, n). The estimations of the parameter at unmeasured points within polygon V_i are the measured value at the nearest single sampled data point x_i that is $\hat{z}(x_0)$ = z(x_i). The weights are:

$$\lambda_i = \begin{cases} 1 & if\ x_i \epsilon V_i, \\ 0 & otherwise \end{cases} \quad (3)$$

All locations (or points) inside each polygon are assigned as similar value [37]. There are several algorithms exist to generate the polygons [36].

Inverse distance weighted (IDW) is deterministic interpolation method widely used in spatial modelling. This method predict the values of a parameter at unsampled location using inverse function of the distance from the point of interest to the sampled points as weighted on linear combination of values at sampled points. Sampled points closer to the unsampled point are more similar to it than those further away in their values assumption is used [36]. The prediction is calculated based on weighted averages, which are proportional to the inverse of the distance between the interpolated and measured points [38]. The weights can be defined as:

$$\lambda_i = \frac{1/d_i^p}{\sum_{i=1}^{n} 1/d_i^p} \quad (4)$$

Here, p is a power parameter, d_i represents the distance between x_0 and x_i, and n is the number of sampled points used for the estimation. The power parameter is the main factor affecting the IDW accuracy. Weights decreases when the distance increases, especially when great value of the power parameter was used. This mean that nearby samples have a heavier weight, more influence on the estimation, and the spatial interpolation is local [39].

Geostatistical methods can be used to describe spatial patterns of the primary parameter, interpolate the values at unsampled locations and model the error or uncertainty of the estimated surface [36]. Kriging algorithms were used for estimating continuous variable in several geostatistics methods. Kriging is a generic name for a generalized least-squares regression algorithms family, used in pioneering work of Danie Krige [40]. The principle of autocorrelation (spatial correlation) between sample data points based on their distance from each other to predict nearby values was used in this geostatistical approach. This autocorrelation in paired sample data points is called semivariogram (γ) and defined as:

$$\gamma(x_i, x_0) = \gamma(h) = \frac{1}{2} var[Z(x_i) - Z(x_0)] \quad (5)$$

Here, Z is parameter value at corresponding data point, h is the point distance between x_i and x_0, and γ(h) is the semivariogram (commonly referred to as variogram) [37,41]. The semivariance can be estimated from the data, as follows:

$$\hat{\gamma}(h) = \frac{1}{2n} \sum_{i=1}^{n} \big(z(x_i) - z(x_i + h)\big)^2 \quad (6)$$

Here, n represent the number of pairs of sample points which separated by distance h. Modelling and estimation of variogram is very important for spatial interpolation. The variogram models could be consist of simple models (i.e. Nugget, Exponential, Spherical, Gaussian, Linear, and Power model) or the nested sum of one or more simple models [42]. Variants of the basic equation (7) used by all kriging estimators, which is a slight modification of equation (2), as follows:

$$\hat{Z}(x_0) - \mu = \sum_{i=1}^{n} \lambda_i [Z(x_i) - \mu(x_0)] \quad (7)$$

Here, μ represent known stationary mean which calculated as the average of the data and assumed to be constant over the whole domain, λ_i is kriging weight, n is the number of sampled points used to make prediction which also depends on the size of the search window, and $\mu(x_0)$ represent the mean of samples within the search window [36]. The ordinary kriging (OK) estimates the parameter values using equations (6) and (7) by replacing μ with a local mean $\mu(x_0)$ or the mean of samples within the search window, and forcing $[1 - \sum_{i=1}^{n} \lambda_i] = 0$, that is $[\sum_{i=1}^{n} \lambda_i] = 0$, which is achieved by plugging it into equation (7). Therefore, equations (6) and (2) generally used by OK to make the estimation [36].

When regression kriging (RK) applied, trend and residuals predictions are made separately and then added back together. Thus, the CDD at a new unmeasured point, x, is predicted using RK as follows [43]:

$$\hat{Z}_{RK}(x) = m(x) + r(x) \quad (8)$$

Here the trend, m(x), is fitted using linear regression analysis and the residuals, r(x), are estimated using OK. The trend model coefficients can be solved using a weighted linear regression, where the covariance matrix, i.e. covariances between sample point pairs, is employed as the matrix of weights. The most known factors that influence on predicted parameter trend should be chosen as independent variables to model the trend [43]. In this study, CDD from CHIRPS data used as independen variable and observed CDD from BMKG network used as dependen variable.

Cross validation applied by testing the estimation method at the locations of existing samples (observed station). The observed CDD value at a particular location is temporarily discarded from the sample data set, then the CDD value at the same location is estimated using the remaining samples. This procedure, can be seen as an experiment the estimation process by pretending that sampled at certain location are not available. After the CDD is predicted, the estimate result then compared it to the true sample value that was initially removed from

the sample data set. This procedure is repeated for all available samples [39]. The resulting true and estimated values can then be compared using several statistical parameters such as correlation coefficient (CC), mean absolute error (MAE) and Root Mean Square Error (RMSE).

Another tool used to compare the different methods is the box plot [44]. This tool used for representing a frequency distribution of cross validation interpolation result. The plain box and whisker diagram consist of a box enclosing the interquartile range values, a line which showing the median and whiskers lines. This whiskers lines extending from the limits of the interquartile range to the extremes of the data, or to some other values such as the 90th percentiles. The brief overview of data distribution, how it lies about the mean or median and extreme values identification could be obtained from box plot [37].

Spatial interpolation performance also plotted using Taylor diagrams [45] which provide a way of graphically summarizing how closely a modelled pattern (or a set of patterns) matches observed values. The similarity between observed and interpolated value for each station are quantified by their correlation coefficient (CC), centered root-mean-square difference (RMSD) and the amplitude of their variations (represented by their standard deviations). This diagram is especially useful in evaluating complex models, such as those used to study geophysical phenomena [45].

3. Results and Discussion

3.1. Spatial Variability of Precipitation Extreme

High resolution precipitation extreme dataset was produced yearly for all time period.

Comparison between maximum CDD calculated based on observational network and gridded CHIRPS data can be seen in Figure 2.

Longest consecutive dry days number explained by color bar. Spatial distribution pattern of CHIRPS and observational based maximum consecutive dry days over the region during analysis period are visually quite similar.

Relatively longer CDD period (140 – 260 days) observed in south western part of the region and another part dominated by shorter CDD (80 – 140 days).

Different perspective arises when more detailed investigation is performed on comparison between observed and CHIRPS value.

CHIRPS based CDD shows shorter period (60 – 120 days) compared to observed value (underestimate) for all region. Relatively high spatial CDD variability between one particular region with another observed by gauged station are not well represented by CHIRPS data. Spatial variability of observed CDD between south eastern part and northern part also not well captured by this dataset. Further investigation applied on yearly average CDD, which shows relatively similar result with maximum CDD with smaller values (Figure 2). CHIRPS generally produced underestimates CDD values and its spatial variability are suppressed.

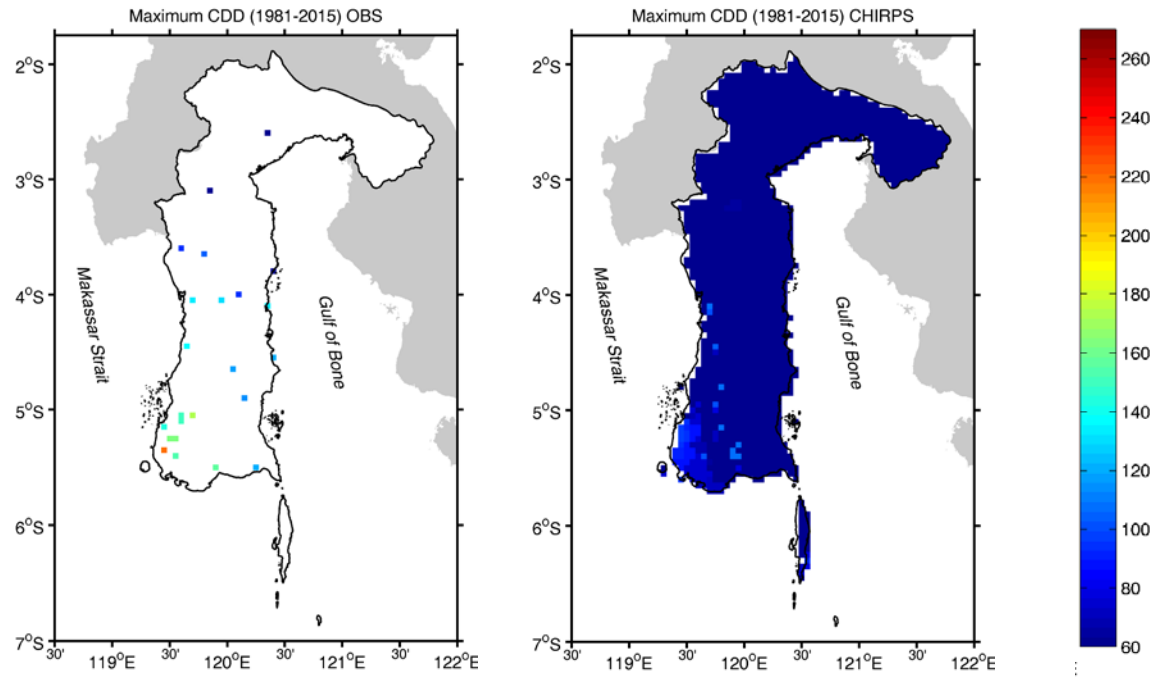

(a) (b)

Figure 2: Comparison of maximum Consecutive Dry Days (CDD) based on gauged observation (a) and CHIRPS data (b) during 35 years period (1981 – 2015). Blue to red shaded explain number of CDD in days unit.

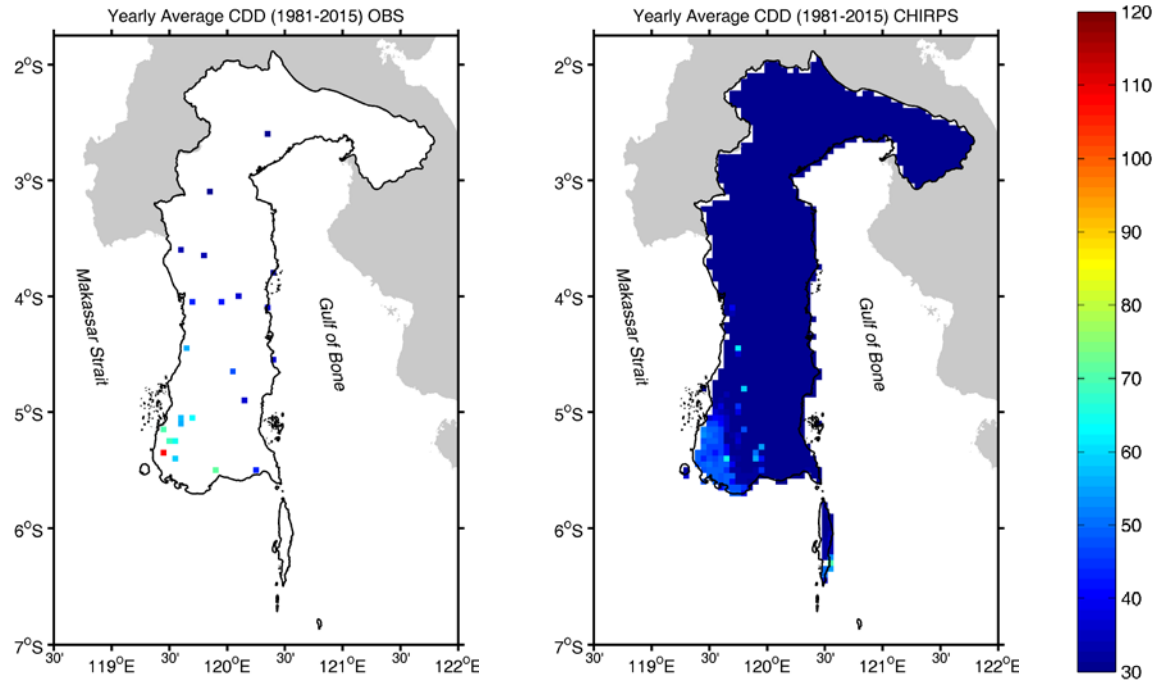

(a) (b)

Figure 3: Comparison of Consecutive Dry Days (CDD) yearly average based on gauged observation (a) and CHIRPS (b) during 35 years period (1981 – 2015). Blue to red shaded explain number of CDD in days unit.

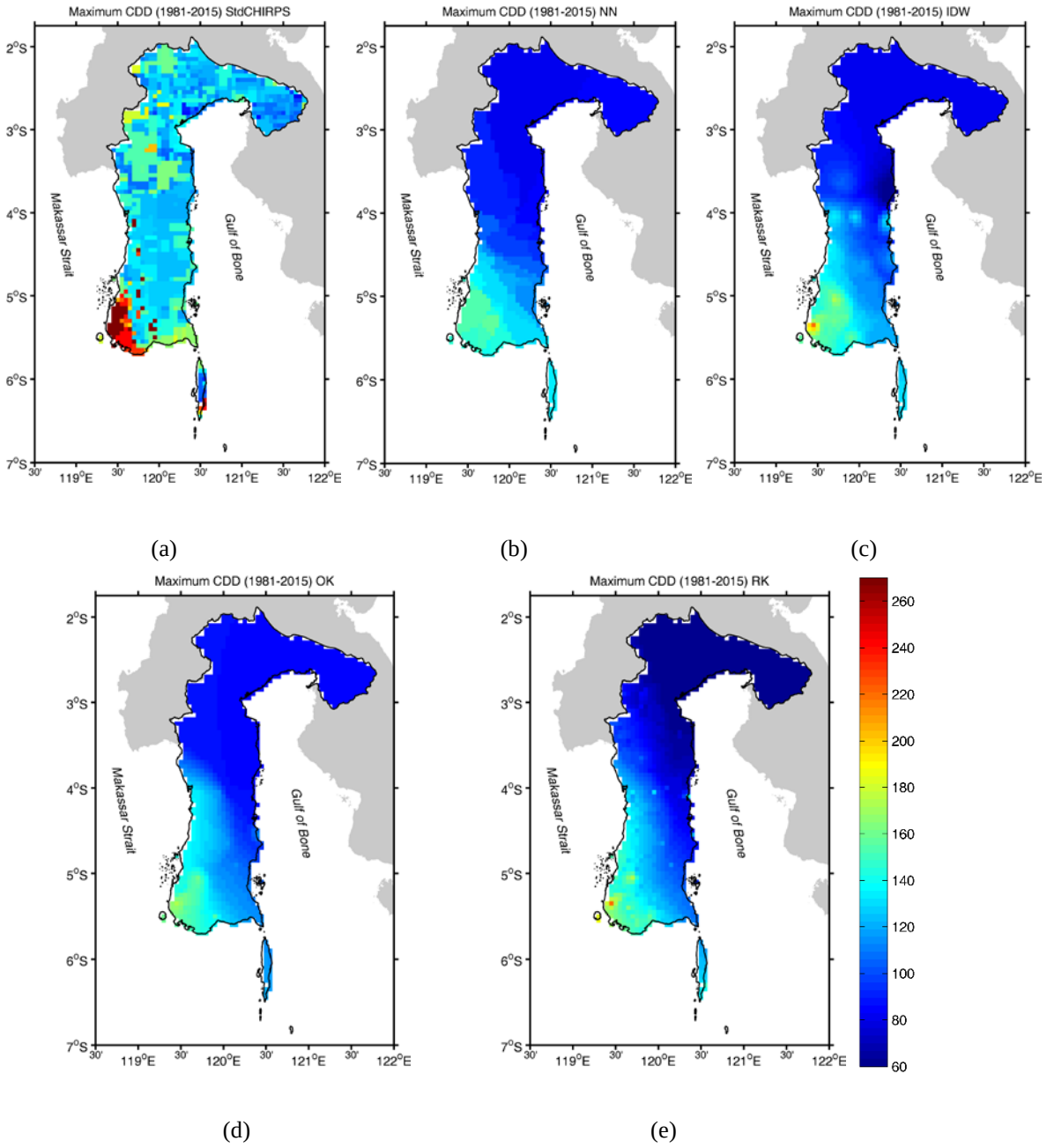

Figure 4: Spatial distribution of maximum CDD based on CHIRPS standardization (Std_CHIRPS) (a), Nearest Neighbours (NN) (b), Invers Distance Method (IDW) (c), Ordinary Kriging (OK) (d) and Regression Kriging (RK) (e) spatial interpolation method. Blue to red shaded explain number of CDD in days unit.

Spatial distribution of maximum CDD based on each interpolation method can be seen in Figure 4. Spatial variability between one region to another can be found easily in this interpolation result. Std_CHIRPS, IDW and RK shows relatively similar higher CDD values in south western part, east part and northern part of the region. These characteristics are not well captured by NN and OK due to the nature of interpolation method which influenced by different nearby observation value. There is no different spatial variability pattern found when using yearly CDD average data (Figure 5).

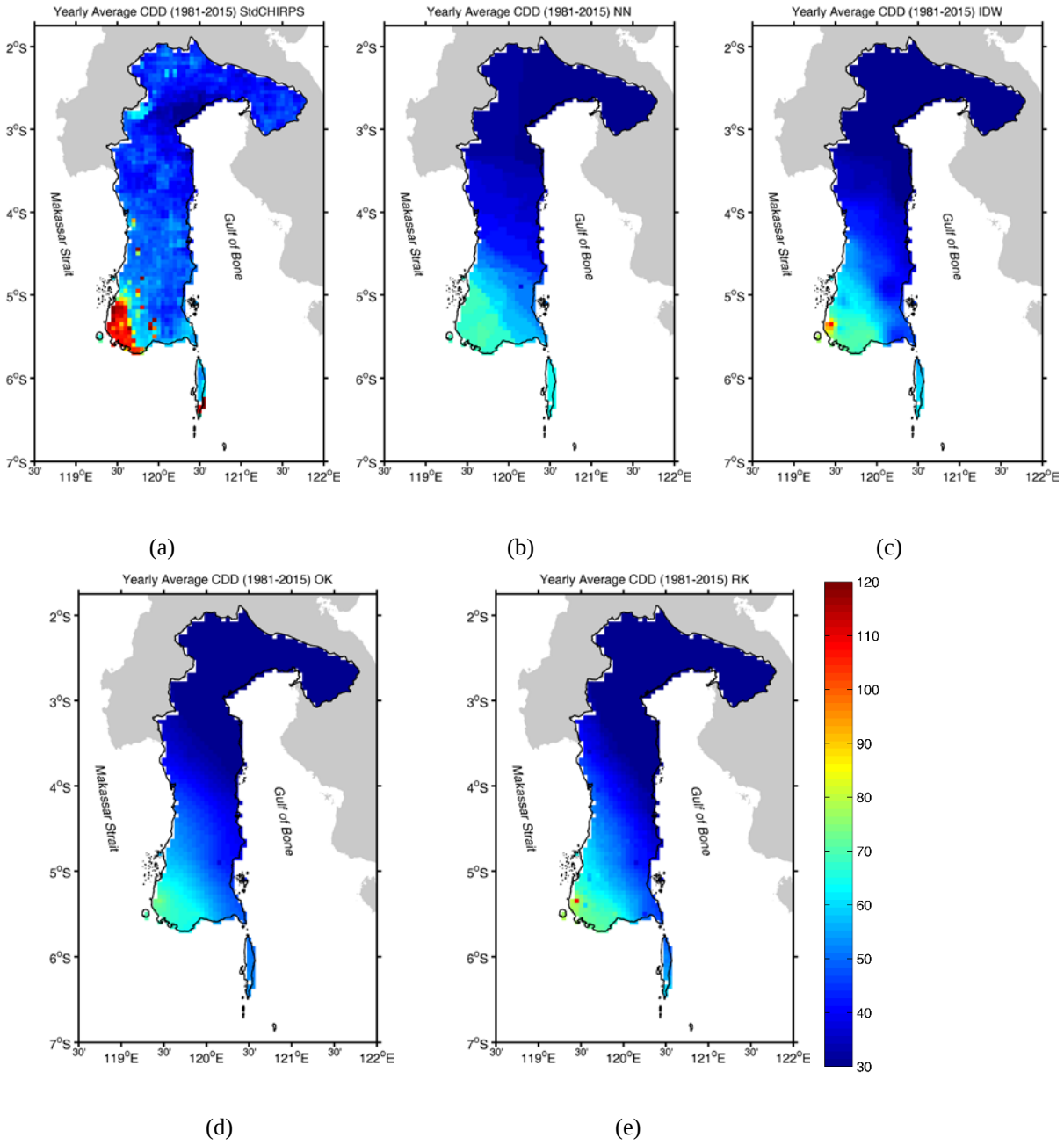

Figure 5: Spatial distribution of yearly average CDD based on Std_CHIRPS (a), NN (b), IDW (c), OK (d) and RK (e) spatial interpolation method. Blue to red shaded explain number of CDD in days unit.

3.2. Spatio – Temporal Performance of Interpolation

Spatial and temporal assessment for each interpolation performance was done by applied leave one out cross validation method with actual CDD from observed station data. Spatial and temporal distribution of CDD in this region are well described by almost all interpolation method, except Std_CHIRPS. Temporal cross validation result of Root Mean Squared Error/ RMSE for each interpolation method can be seen on Figure 6. Interpolation performance generally reduced during La Niña periods or after El Niño years for all method. This condition occurred due to smaller CDD value over all region during this period which reduce spatial variability.

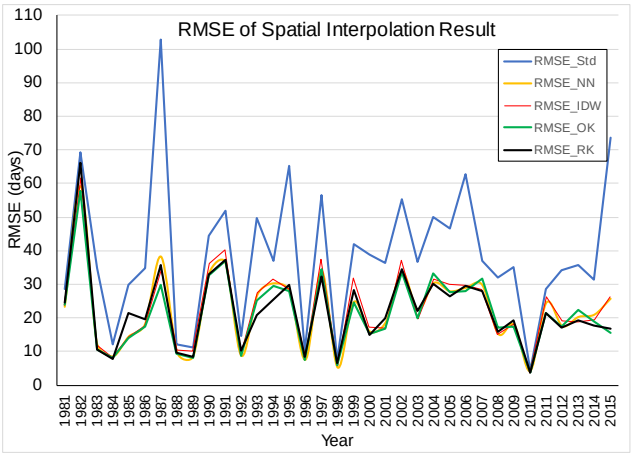

(a)

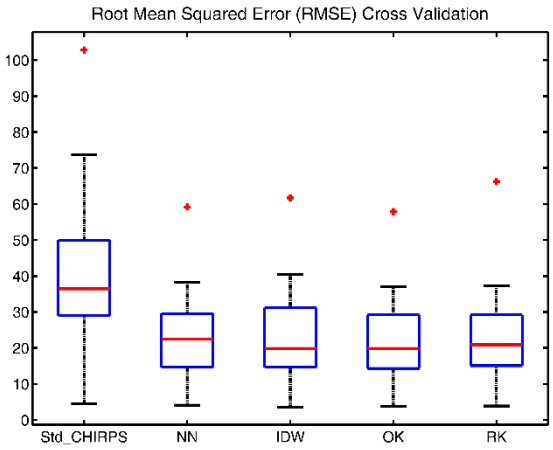

(d)

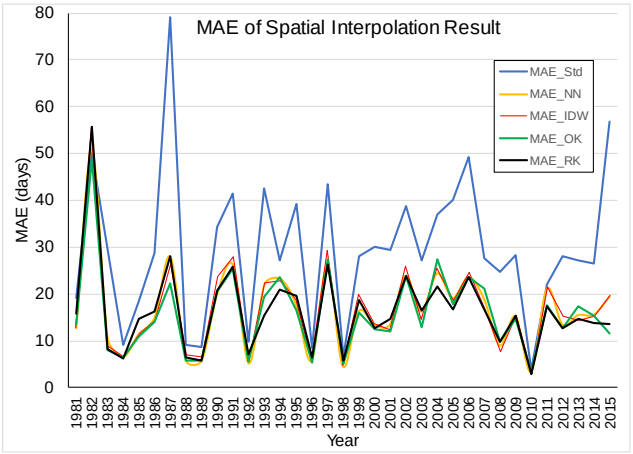

(b)

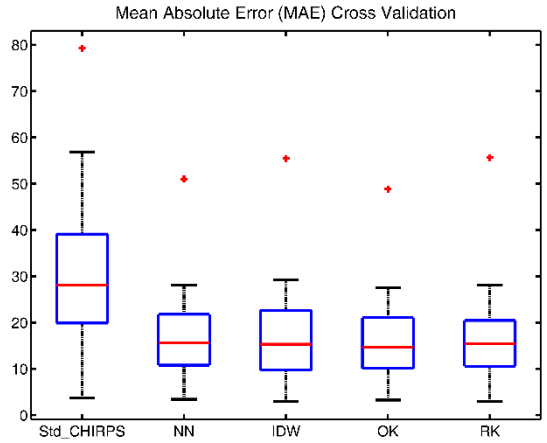

(e)

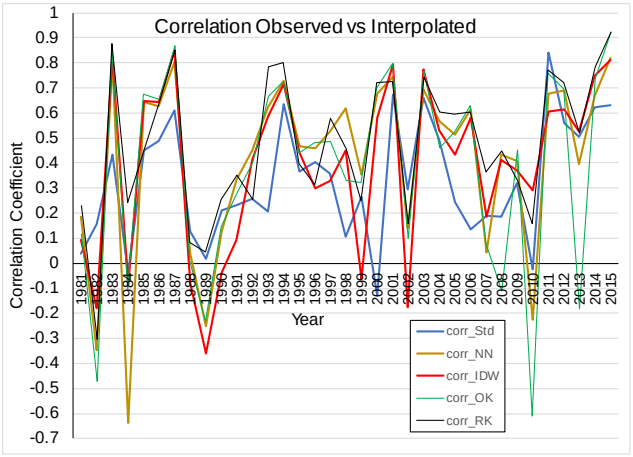

(c)

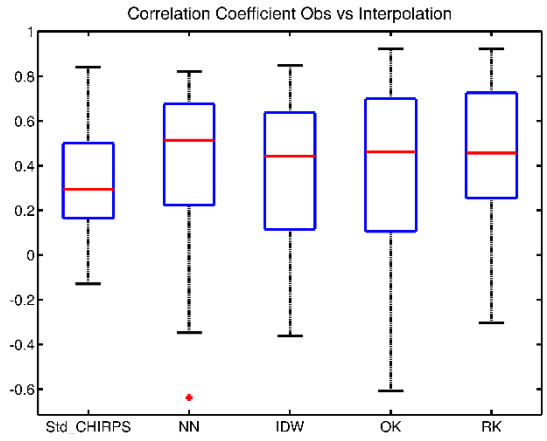

(f)

Figure 6: Temporal Cross Validation Result of Root Mean Squared Error/ RMSE (a), Mean Absolute Error/ MAE (b), Correlation Coefficient (c) and box plot of each parameter (d, e, f) for CHIRPS standardization (Std_CHIRPS), Nearest Neighbour (NN), Invers Distance Method (IDW), Ordinary Kriging (OK) and Regression Kriging (RK) Spatial Interpolation Method

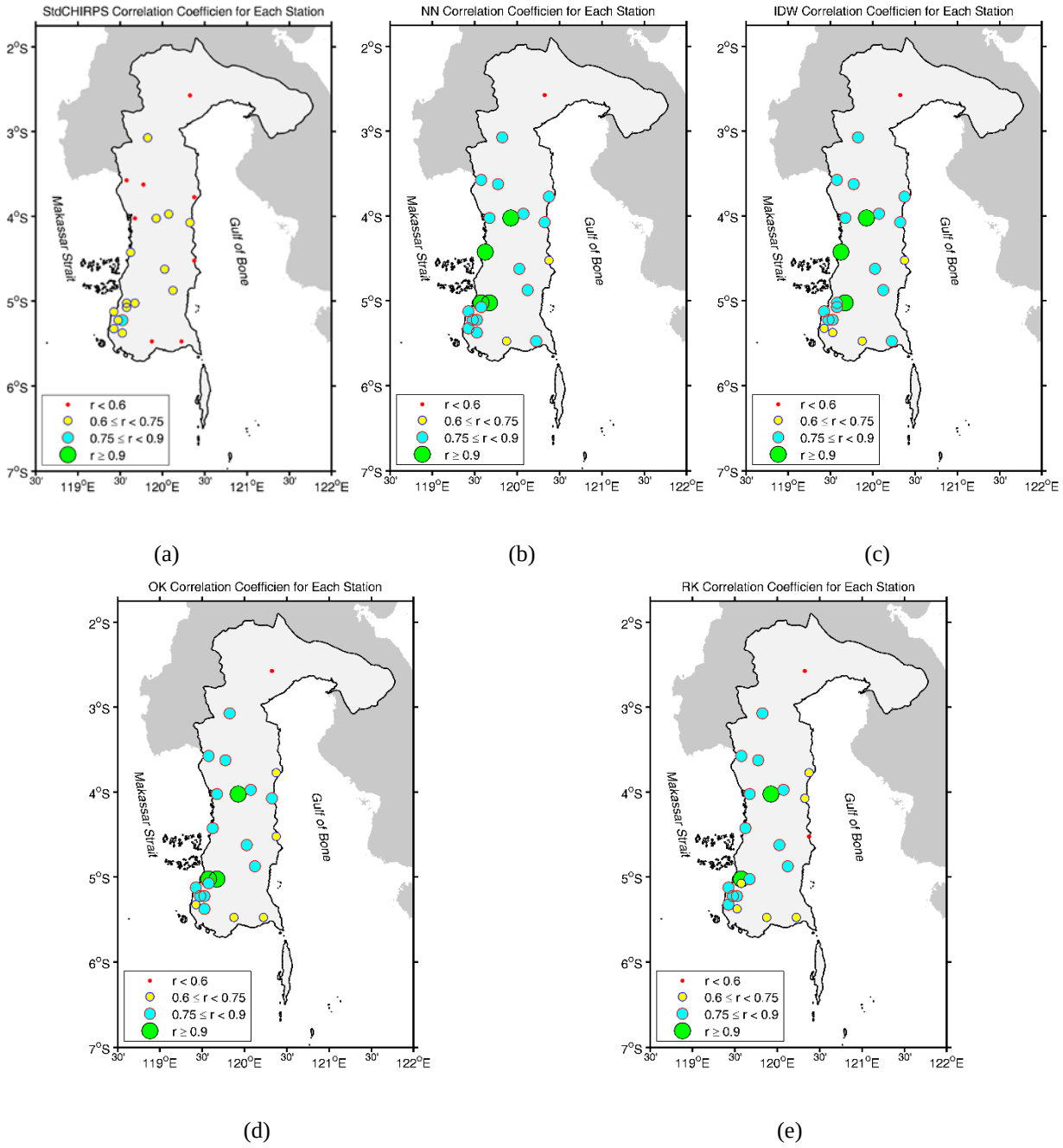

Figure 7: Spatial map of cross validation result showed by coefficient correlation values for Std_CHIRPS (a), NN (b), IDW (c), OK (d) and RK (e) spatial interpolation method.

Spatial map of cross validation result expressed by coefficient correlation value are showed in Figure 7. Relatively low correlation value observed on northern and southern part of the region. Meanwhile, in the center of the region generally shows higher interpolation performance. Limited nearby station for interpolation process in the northern and southern part suspected as reason for this occurrence. Smaller coefficient values found over all region when Std_CHIRPS applied. This condition expected caused by standardization process on CHIRPS data which intensify standard deviation value.

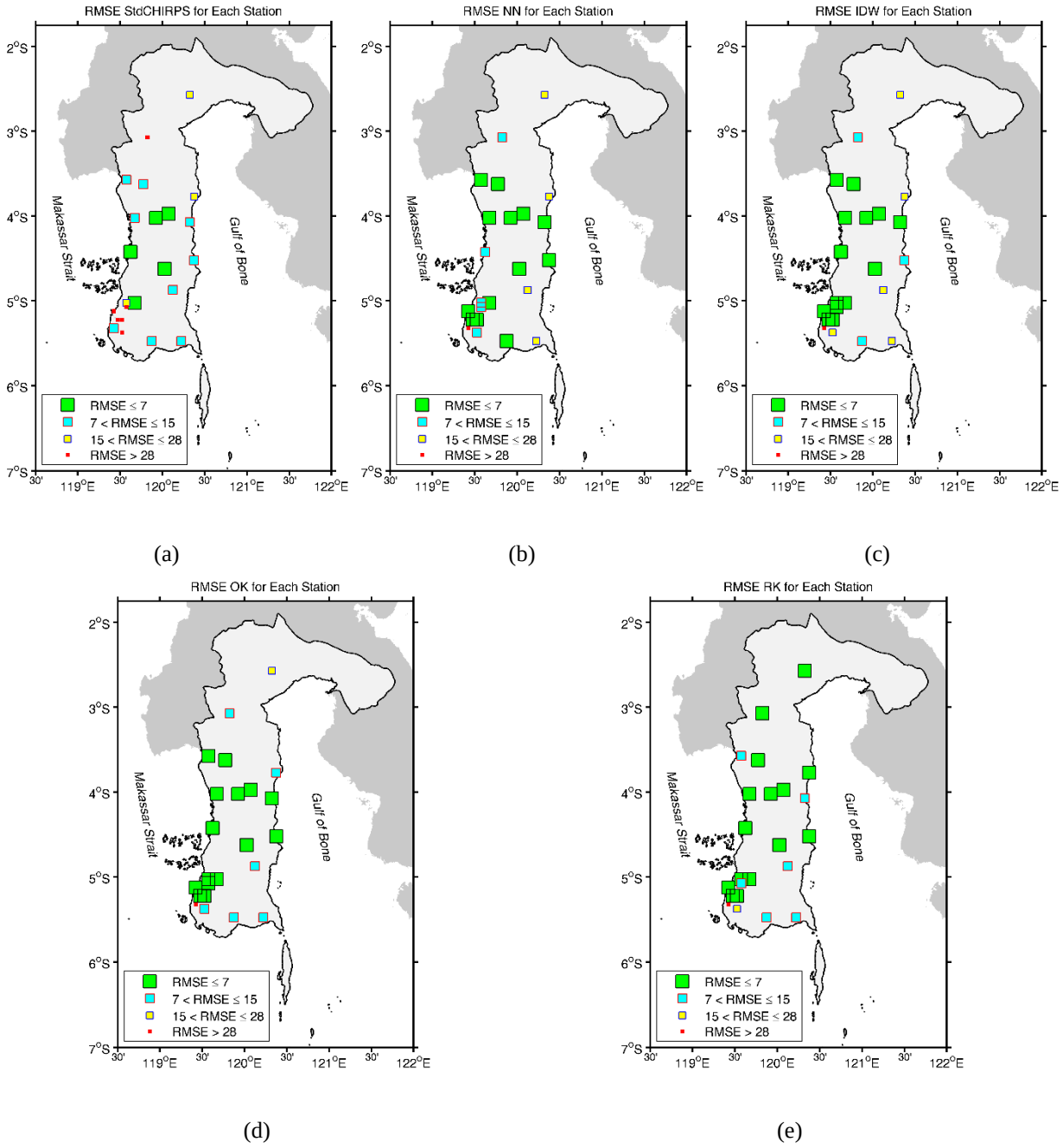

Figure 8: Spatial map of cross validation result showed by root mean square error (RMSE) values for Std_CHIRPS (a), NN (b), IDW (c), OK (d) and RK (e) spatial interpolation method.

Spatial map of cross validation result described using root mean square error (RMSE) values for each interpolation method can found in Figure 8.

Relatively similar result found when interpretation performance assessed using RMSE value. Smaller RMSE value generally located at the center of the region which have more nearby station used for interpolation process. Utilization of CHIRPS data as second variable for interpolation method enhanced RK performance by reducing RMSE value, especially in the northern part of the region.

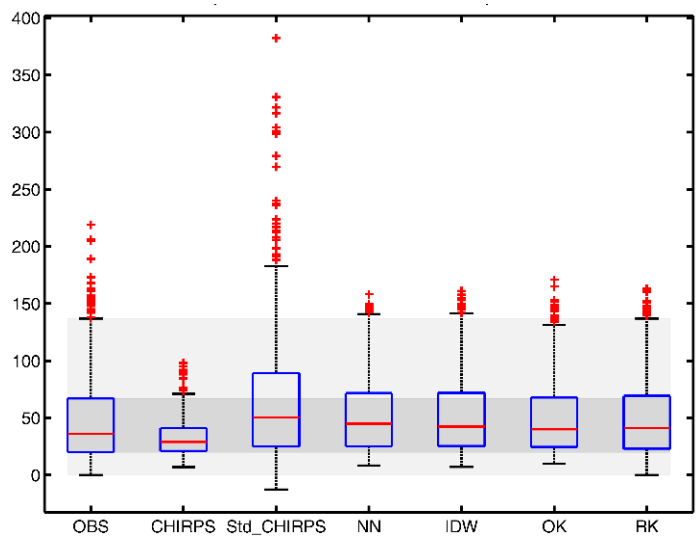

Figure 9: Box plot comparison between Observed CDD (OBS), original CHIRPS data (CHIRPS), CHIRPS standardization (Std_CHIRPS), Nearest Neighbour (NN), Invers Distance Method (IDW), Ordinary Kriging (OK), Regression Kriging (RK) spatial interpolation method. Shaded area shows observed CDD range and interquartile range (darker) as observed trace hold comparison.

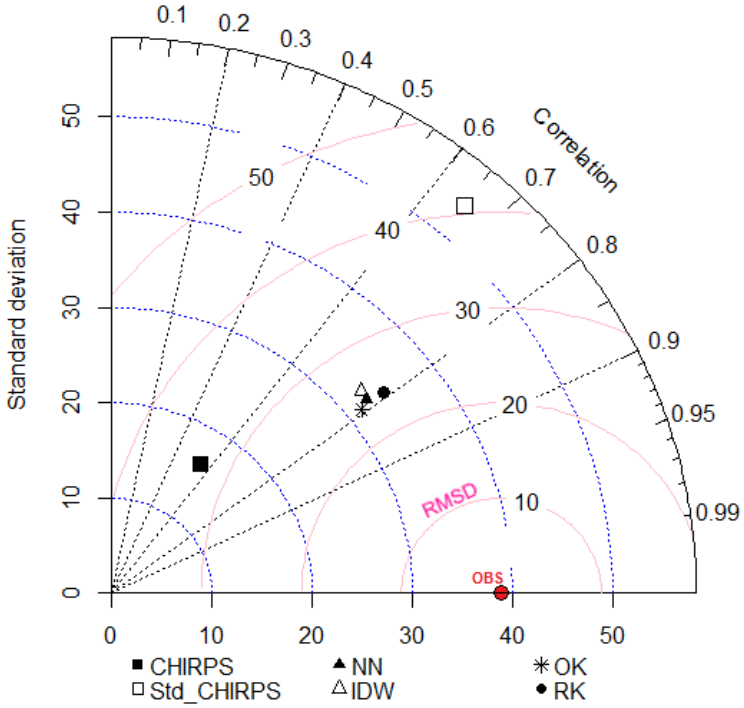

Figure 10: Taylor diagram of spatio – temporal cross validation result for all years and all observation point. Dotted black line denote correlation coefficient, RMSE for red line, and dotted blue line for standard deviation.

Box plot comparison between observed CDD (OBS) and another interpolation method can be seen in Figure 9. Spatial and temporal distribution of observed CDD in this region are well described by almost all interpolation method, except original CHIRPS data and Std_CHIRPS. CHIRPS tend to have smaller inter quartile range,

while Std_CHIRPS have wider distribution result with generate more upper extreme value. Relatively high correlation coefficient value (r = 0.79) with lowest RMSE obtained by geostatistical approach (OK=23.8; RK =24.1) can be seen on Figure 10. Nevertheless, RK shows fitted interquartile range and closest standard deviation value (32.3) compared to observation data (38.9) (Figure 8).

These results are consistent with previous studies [10,32] which confirmed superiority performance of geostatistics approach for precipitation estimation in archipelagic regions with prominent climate variability. The similar result was also found when spatial interpolation and geostatistical approach applied for soil moisture [46] and land surface temperature estimation [47,48].

4. Conclusion

Spatial and temporal distribution of CDD in South Sulawesi region are well described by almost all interpolation method, except Std_CHIRPS (high RMSE and MAE fluctuation). Cross validation was applied on interpolated CDD data against observed value over 35 years period. Interpolation performance reduced during La Niña periods or after El Niño years. This condition occurred due to highly spatial climate variability and various spatial climate response to global climate anomaly between one location to another, especially on eastern and western part of South Sulawesi. Geostatistical approach shows its superiority against simple statistics standardization with observation technique and spatial interpolation method when applied to CDD data. Relatively high correlation coefficient value (r = 0.79) with lowest RMSE obtained by geostatistical approach (OK=23.8; RK =24.1). Nevertheless, RK shows fitted interquartile range and closest standard deviation value (32.3) compared to observation data (38.9). This result makes RK becomes the best interpolation method for CDD in South Sulawesi.

Acknowledgements

This research is part of first author PhD Dissertation thesis on Applied Climatology at Graduate School of Bogor Agricultural University (IPB). The authors would like to thank Indonesia Agency for Meteorology Climatology and Geophysics (BMKG) for providing a scholarship for first author PhD program and providing the observation data used on this research.

References

[1] T. B. McKee, N. J. Doesken, and J. Kleist, “Drought Monitoring with Multiple Time Scales,” in Proceedings of the 9th AMS Conference on Applied Climatology, 1995, pp. 233–236.

[2] S. Beguería, S. M. Vicente-Serrano, F. Reig, and B. Latorre, “Standardized precipitation evapotranspiration index (SPEI) revisited: Parameter fitting, evapotranspiration models, tools, datasets and drought monitoring,” Int. J. Climatol., vol. 34, no. 10, pp. 3001–3023, 2014.

[3] Y. Duan, Z. Ma, and Q. Yang, “Characteristics of consecutive dry days variations in China,” Theor. Appl. Climatol., pp. 1–9, 2016.

[4] A. M. G. K. Tank, F. W. Zwiers, and X. Zhang, Guidelines on Analysis of Extremes in a Changing Climate in Support of Informed Decisions for Adaptation, TD No 1500., no. WCDMP-No.72. Geneva, Switzerland: World Meteorological Organization, 2009.

[5] D. Gunawan, G. Gravenhorst, D. Jacob, and R. Podzun, "Rainfall variability studies in South Sulawesi using Regional Climate Model REMO," J. Meteorol. dan Geofis., vol. 4, pp. 65–70, 2003.

[6] A. M. Setiawan, "Mapping of South Sulawesi Rainfall Distribution using Arcview GIS [in Indonesian]," Makassar State University (UNM), Makassar, 2007.

[7] J.-I. Hamada, M. D. Yamanaka, J. Matsumoto, S. Fukao, P. A. Winarso, and T. Sribimawati, "Spatial and Temporal Variations of the Rainy Season over Indonesia and their Link to ENSO," J. Meteorol. Soc. Japan. Ser. II, vol. 80, no. 2, pp. 285–310, 2002.

[8] P. Cantet, "Mapping the mean monthly precipitation of a small island using kriging with external drifts," Theor. Appl. Climatol., vol. 127, no. 1–2, pp. 31–44, 2017.

[9] D. Ozturk and F. Kilic, "Geostatistical approach for spatial interpolation of meteorological data," An Acad Bras Cienc (Annals Brazilian Acad. Sci., vol. 88, no. 884, pp. 2121–2136, 2016.

[10] S. K. Adhikary, N. Muttil, and A. G. Yilmaz, "Cokriging for enhanced spatial interpolation of rainfall in two Australian catchments," Hydrol. Process., vol. 31, no. 12, pp. 2143–2161, 2017.

[11] A. M. Setiawan, W. S. Lee, and J. Rhee, "Spatio-temporal characteristics of Indonesian drought related to El Niño events and its predictability using the multi-model ensemble," Int. J. Climatol., vol. 37, no. 13, pp. 4700–4719, 2017.

[12] A. M. Setiawan, Y. Koesmaryono, A. Faqih, and D. Gunawan, "Utilization of near real-time NOAA-AVHRR satellite output for El Niño induced drought analysis in Indonesia (Case study : El Niño 2015 induced drought in South Sulawesi)," Int. J. Remote Sens. Earth Sci., vol. 13, no. 2, pp. 87–94, 2016.

[13] M. Martono and T. Wardoyo, "Impacts of El Niño 2015 and the Indian Ocean Dipole 2016 on rainfall in the Pameungpeuk and Cilacap regions," Forum Geogr., vol. 31, no. 2, Dec. 2017.

[14] L. S. Supriatin and M. Martono, "Impacts of Climate Change (El Nino, La Nina, and Sea Level) on the Coastal Area of Cilacap Regency," Forum Geogr., vol. 30, no. 2, pp. 106–111, 2016.

[15] S. Lestari, J.-I. Hamada, F. Syamsudin, Sunaryo, J. Matsumoto, and M. D. Yamanaka, "ENSO influences on rainfall extremes around Sulawesi and Maluku islands in the eastern Indonesian Maritime Continent," SOLA, vol. 12, no. 1, pp. 37–41, 2016.

[16] F. Kogan, W. Guo, A. Strashnaia, A. Kleshenko, O. Chub, and O. Virchenko, "Modelling and prediction of crop losses from NOAA polar-orbiting operational satellites," Geomatics, Nat. Hazards

Risk, vol. 7, no. 3, pp. 886–900, 2015.

[17] C. Toté, D. Patricio, H. Boogaard, R. van der Wijngaart, E. Tarnavsky, and C. Funk, "Evaluation of satellite rainfall estimates for drought and flood monitoring in Mozambique," Remote Sens., vol. 7, no. 2, pp. 1758–1776, 2015.

[18] Q. Dai, D. Han, and L. Zhuo, "Seasonal ensemble generator for radar rainfall using copula and autoregressive model," 2015.

[19] R. R. E. Vernimmen, A. Hooijer, Mamenun, E. Aldrian, and A. I. J. M. Van Dijk, "Evaluation and bias correction of satellite rainfall data for drought monitoring in Indonesia," Hydrol. Earth Syst. Sci., vol. 16, no. 1, pp. 133–146, Jan. 2012.

[20] M. E. Moeletsi and S. Walker, "Evaluation of NASA satellite and modelled temperature data for simulating maize water requirement satisfaction index in the Free State Province of South Africa," Phys. Chem. Earth, vol. 50–52, pp. 157–164, 2012.

[21] J. L. Peña-Arancibia, A. I. J. M. van Dijk, L. J. Renzullo, and M. Mulligan, "Evaluation of Precipitation Estimation Accuracy in Reanalyses, Satellite Products, and an Ensemble Method for Regions in Australia and South and East Asia," J. Hydrometeorol., vol. 14, no. 4, pp. 1323–1333, 2013.

[22] C. Dyn, "Precipitation climatology over India : validation with observations and reanalysis datasets and spatial trends," Clim. Dyn., 2015.

[23] J. Kim and J. H. Ryu, "A heuristic gap filling method for daily precipitation series," Water Resour. Manag., vol. 30, no. 7, pp. 2275–2294, 2016.

[24] B. Jongjin, P. Jongmin, R. Dongryeol, and C. Minha, "Geospatial blending to improve spatial mapping of precipitation with high spatial resolution by merging satellite-based and ground-based data," Hydrol. Process., vol. 30, no. 16, pp. 2789–2803, 2016.

[25] C. Funk et al., "The climate hazards infrared precipitation with stations—a new environmental record for monitoring extremes," Sci. Data, vol. 2, p. 150066, Dec. 2015.

[26] U. Schneider, A. Becker, M. Ziese, and B. Rudolf, "Global Precipitation Analysis Products of the GPCC," pp. 1–13, 2012.

[27] A. Becker et al., "A description of the global land-surface precipitation data products of the Global Precipitation Climatology Centre with sample applications including centennial (trend) analysis from 1901-present," Earth Syst. Sci. Data, vol. 5, no. 1, pp. 71–99, Feb. 2013.

[28] A. Yatagai, O. Arakawa, K. Kamiguchi, and H. Kawamoto, "A 44-Year Daily Gridded Precipitation Dataset for Asia," Sola, vol. 5, pp. 3–6, 2009.

[29] A. Yatagai, K. Kamiguchi, O. Arakawa, A. Hamada, N. Yasutomi, and A. Kitoh, "APHRODITE : Constructing a Long-Term Daily Gridded Precipitation Dataset for Asia Based on a Dense Network of Rain Gauges," Bull. Am. Meteorol. Soc., vol. 93, no. 9, pp. 1401–1415, 2012.

[30] J.-J. Wang, R. F. Adler, G. J. Huffman, and D. Bolvin, "An Updated TRMM Composite Climatology of Tropical Rainfall and Its Validation," J. Clim., vol. 27, no. 1, pp. 273–284, 2014.

[31] N. Hofstra, M. Haylock, M. New, P. Jones, and C. Frei, "Comparison of six methods for the interpolation of daily , European climate data," vol. 113, no. November, 2008.

[32] J. Q. Basconcillo et al., "Evaluation of spatial interpolation techniques for operational climate monitoring in the Philippines," SOLA, vol. 13, no. 0, pp. 114–119, 2017.

[33] Yanto, B. Livneh, and B. Rajagopalan, "Development of a gridded meteorological dataset over Java island, Indonesia 1985-2014," Sci. Data, vol. 4, pp. 1–10, 2017.

[34] L. Haimberger, "Homogenization of radiosonde temperature time series using innovation statistics," J. Clim., vol. 20, no. 7, pp. 1377–1403, 2007.

[35] A. Singh, R. K. Sahoo, A. Nair, U. C. Mohanty, and R. K. Rai, "Assessing the performance of bias correction approaches for correcting monthly precipitation over India through coupled models," Meteorol. Appl., vol. 24, no. 3, pp. 326–337, 2017.

[36] J. Li and A. D. Heap, A Review of Spatial Interpolation Methods for Environmental Scientists, Geoscience. Canberra: Geoscience Australia, 2008.

[37] R. Webster and M. A. Oliver, Geostatistics for Environmental Scientists, Second Edi., no. 2. Chichester: John Wiley & Sons Ltd, 2007.

[38] D. Shepard, "A two-dimensional interpolation function for irregularly-spaced data," Proc. 1968 23rd ACM Natl. Conf., pp. 517–524, 1968.

[39] E. H. Isaaks and R. M. Srivastava, An Introduction to Applied Geostatistics. New York: Oxford University Press, 1989.

[40] D. G. Krige, "A statistical approach to some basic mine valuation problems on the Witwatersrand," Journal of the Chemical, Metallurgical and Mining Society of South Africa, vol. 52, no. 6. pp. 201–215, 1952.

[41] M. A. Oliver and R. Webster, "A tutorial guide to geostatistics: Computing and modelling variograms and kriging," Catena, vol. 113, pp. 56–69, 2014.

[42] N. A. C. Cressie, Special Topics in Statistics for Spatial Data, Revised Ed. New York: John Wiley &

Sons, Inc, 1993.

[43] F. J. Moral, “Comparison of different geostatistical approaches to map climate variables: Application to precipitation,” Int. J. Climatol., vol. 30, no. 4, pp. 620–631, 2010.

[44] T. J. W. McGrill R. and W. A. Larsen, “Variations of box plots,” Am. Stat., vol. 32, no. 1, pp. 12–16, 1978.

[45] K. E. Taylor, “Summarizing multiple aspects of model performance in a single diagram,” J. Geophys. Res. Atmos., vol. 106, no. D7, pp. 7183–7192, 2001.

[46] S. Yuan and S. M. Quiring, “Comparison of three methods of interpolating soil moisture in Oklahoma,” Int. J. Climatol., vol. 37, no. 2, pp. 987–997, 2017.

[47] Q. Wang, V. Rodriguez-Galiano, and P. M. Atkinson, “Geostatistical solutions for downscaling remotely sensed land surface temperature,” Int. Arch. Photogramm. Remote Sens. Spat. Inf. Sci. - ISPRS Arch., vol. 42, no. 2W7, pp. 913–917, 2017.

[48] T. Hengl, G. B. M. Heuvelink, M. P. Tadić, and E. J. Pebesma, “Spatio-temporal prediction of daily temperatures using time-series of MODIS LST images,” Theor. Appl. Climatol., vol. 107, no. 1–2, pp. 265–277, 2012.